

**LANDAU THEORY OF FERROELECTRIC  
THIN FILMS AND SUPERLATTICES**

**ONG LYE HOCK**

**UNIVERSITI SAINS MALAYSIA  
2004**

**LANDAU THEORY OF FERROELECTRIC  
THIN FILMS AND SUPERLATTICES**

**by**

**ONG LYE HOCK**

**March 2004**

**Thesis submitted in fulfillment of the requirements  
for the degree of Doctor of Philosophy**

## **ACKNOWLEDGEMENTS**

I sincerely express my heartfelt gratitude and appreciation to my supervisors, Prof. David Reginald Tilley and Prof. Junaidah Osman for their high level of professional supervision and guidance during the whole duration of my research. Their continuous motivation and encouragement as well as their tireless efforts in their commitment have greatly inspired me to accomplish this project. For their assistance, patience and concerns in supervising my work, I am indebted to them.

For my own family, I am indebted to them too; especially my wife, Lim Ah Suan, who has been so patient and tolerant all this while. My three children likewise are always obedient and understanding; and they have spared me time for this study. Without the constant support and encouragement from all of them, it would have been impossible to accomplish this study.

# TEORI LANDAU BAGI SELAPUT NIPIS DAN SUPERKEKISI FEROELEKTRIK

## ABSTRAK

Teori Landau Devonshire (LD) bagi peralihan fasa dalam feroelektrik (FE) telah digunakan di dalam pengajian kami berkenaan ciri-ciri selaput nipis dan dwilapis atau superkekisi. Teori ini digunakan dalam pengajian selaput nipis FE tertib kedua yang telah diubahsuaikan oleh Tilley dan Zeks; di mana ungkapan perubahan dalam ruang  $|\nabla P|^2$  dan panjang tentuan-luar permukaan  $\delta$  telah dimasukkan. Nilai positif bagi  $\delta$  bermakna pengkutuban menyusut pada permukaan dan nilai negatif  $\delta$  bermakna pengkutuban meningkat di permukaan. Kami telah perolehi ungkapan yang lebih mudah bagi profil pengkutuban berbanding dengan ungkapan yang telah diterbitkan terlebih dahulu dan keputusan kami telah memberikan penjelasan kepada dua percanggahan yang terdapat dalam literatur. Pertama, perubahan fasa peringkat awal dalam selaput nipis FE tertib kedua yang telah diramalkan oleh satu kajian terlebih awal tidak didapati didalam perhitungan kami; dan kedua, pernyataan hasil kajian Qu *et al.* bahawa terdapat peralihan fasa tertib pertama didalam selaput nipis FE yang berbahan tertib kedua ternyata tidak benar melalui pelbagai cara perhitungan kami. Fungsi termodinamik dan persandaran suhu bagi ketebalan kritikal juga telah dihitungkan secara analitik. Ungkapan LD bagi FE pukal tertib pertama dan tertib kedua juga

digunakan untuk memodelkan dwilapis FE bahan tertib pertama dan tertib kedua. Dianggapkan bahawa lapisan perantaraan menghasilkan gandingan antiferoelektrik di antara dua selaput bagi dwilapis ini. FE ini diselidik dengan menganggap beberapa kemudahan; ia itu bahan untuk setiap lapisan dianggapkan sama jenis dan purata pengkutuban di dalam setiap lapisan dianggapkan seragam. Lengkungan litup dielektrik histeresis (DHL) bagi kedua-dua model dwilapis disurihkan dengan menyelesaikan ungkapan tenaga bebas LD pada keadaan keseimbangan secara berangka. Bagi dwilapis-dwilapis tertib pertama dan tertib kedua yang mempunyai nisbah ketebalan tak serupa, corak DHL yang berbagai dapat diperolehi dengan mengubah nisbah ketebalan  $l$ , pemalar gandingan antara subkekisi  $j$  dan suhu  $t$ . DHL yang mempunyai enam lengkung litup bagi dwilapis-dwilapis tertib pertama dapat direkabentukkan melalui pemilihan nilai-nilai kecil  $l$  dan  $j$  yang sesuai dalam julat suhu  $t_{SH} < t < t_2$  yang melebihi suhu genting pukal  $t_{CB}$ . Ungkapan tenaga bebas bagi antiferoelektrik (AFE) pukal tertib pertama dan tertib kedua adalah serupa dengan ungkapan model kami apabila ketebalan bagi setiap lapisan dalam dwilapis-dwilapis itu dianggapkan sama; maka keputusan kami dapat diaplikasikan untuk AFE pukal. DHL empat lengkungan litup bagi AFE pukal tertib pertama boleh diperolehi dengan mengubah nilai  $j$  dalam julat suhu  $t_{SH} \leq t < t_2$ . Daripada keputusan-keputusan pengajian kami, ciri-ciri penguisan multi-keadaan dalam model dwilapis-dwilapis tertib pertama dan tertib kedua kami telah ditunjukkan. Namun begitu, kami tidak menyangkal bahawa model yang kami cadangkan itu dapat digunakan untuk pembuatan peranti penguisan; tetapi keputusan-keputusan ini diharap dapat memotivasikan pengkajian yang lebih mendalam untuk menerokakan potensi ini.

## ABSTRACT

The Landau Devonshire (LD) theory of phase transitions in ferroelectrics (FE) is applied to studies of thin films, bilayers and superlattices. The theory applied in the study of second order FE thin films is that of Tilley and Žekš; in which the spatial variation  $|\nabla P|^2$  term and the surface extrapolation length  $\delta$  are incorporated. A positive value of  $\delta$  means polarization is depleted at the surface and negative  $\delta$  means polarization is enhanced. We have obtained much simpler expressions for the polarization profiles compared with the previous work and our results also clarify two discrepancies in the literature. First, the incipient phase transition in the second order FE thin film speculated by Tilley and Žekš is not found in our calculations; and secondly, the claim by Qu *et al.* that there is a first order phase transition in a FE thin film of second order material is refuted through various methods of calculation. Thermodynamic functions and the temperature dependence of the critical thickness of the film are also calculated analytically. The LD bulk first-order and second-order expressions are used to model FE bilayers of first-order and second-order materials. It is assumed that an intermediate layer produces antiferroelectric coupling between the component films of the bilayer. Some simplifications are made: the materials in both layers are taken to be the same and the average polarization in each of the layers is assumed uniform. Dielectric hysteresis loops (DHLs) of the bilayers are drawn by solving the equilibrium states of the LD free energy expressions numerically. For

unequal thickness ratio in both the first-order and second-order bilayers, diverse patterns of DHLs can be obtained by varying the thickness ratio  $l$ , the interlayer coupling constant  $j$  and the temperature  $t$ . Six-loop DHLs of the first order bilayer can be designed by proper choices of small values  $l$  and  $j$  within a certain temperature range  $t_{SH} < t < t_2$  above the bulk critical temperature  $t_{CB}$ . Free energy expressions of the first and second order bulk antiferroelectrics (AFE) are the same as our expressions when the thicknesses of the two layers in the bilayer are taken to be equal; so our results apply also to the bulk AFE. We can obtain quadruple-loop DHLs of the first order bulk AFE by varying  $j$  within temperature range  $t_{SH} \leq t < t_2$ . From the results of our studies, multi-state switching capability is indicated in first order and second order bilayers with antiferroelectric coupling across the interface. However, we do not presume that such switching devices can be made, but the results might motivate more in-depth studies to explore this potential.

## CONTENTS

	<b>Page</b>
<b>ACKNOWLEDGEMENTS</b>	<b>ii</b>
<b>ABSTRAK</b>	<b>iii</b>
<b>ABSTRACT</b>	<b>v</b>
<b>CONTENTS</b>	<b>vii</b>
<b>LIST OF SYMBOLS AND ABBREVIATIONS</b>	<b>xii</b>
<b>CHAPTER 1 AN OVERVIEW</b>	<b>1</b>
1.1 Introduction	1
1.2 Overview of the Thesis	3
<b>CHAPTER 2 GENERAL VIEW ON BULK FERROELECTRICITY</b>	<b>4</b>
2.1 Introduction	4
2.2 Bulk Ferroelectric Properties	5
2.3 Ferroelectric Materials and Their Properties	10
2.3.1 Displacive Ferroelectrics	11
2.3.2 Order-Disorder Ferroelectrics	15
2.4 Theory of Ferroelectric Phase Transitions	18
2.4.1 Soft Mode and Microscopic Theory	19
2.4.2 Landau Devonshire Theory	23
2.5 Applications of Bulk ferroelectrics	31



2.5.1	Applications of Piezoelectric Effects	31
2.5.2	Applications of Dielectric Property	32
2.5.3	Applications of Pyroelectric Effects	33
2.5.4	Applications of Electro-Optic Effects	34
2.5.5	Application of Polarization Reversibility	35

### **CHAPTER 3 REVIEW ON FERROELECTRIC THIN FILMS AND SUPERLATTICES**

		<b>37</b>
3.1	Introduction	37
3.2	Techniques of Fabrication and Results	40
3.2.1	Fabrications of FE thin Films	41
3.2.2	Fabrications of FE Superlattices / Multilayers	46
3.2.3	General Discussion of Fabrication Techniques	48
3.3	Experimental Results on Finite Size Effects of FE Thin Films and Superlattices	51
3.3.1	Experimental Results on Thin Films	52
3.3.2	Experimental Results on Superlattices / Multilayers	57
3.4	Theoretical Results on Finite Size Effects of FE Thin Films and Superlattices	59
3.4.1	Theoretical Results for FE Thin Films	60
3.4.1.1	Landau Devonshire Theory in FE Thin Films	60
3.4.1.2	Ising Model in FE Thin Films	64
3.4.2	Theoretical Results for FE Superlattices	68

<b>CHAPTER 4</b>	<b>LANDAU THEORY OF SECOND ORDER PHASE</b>	
	<b>TRANSITION IN FE THIN FILMS</b>	<b>73</b>
4.1	Introduction	73
4.2	Formalism of Ferroelectric Thin Film	75
4.3	Polarization Profiles of Ferroelectric Thin Films	79
	4.3.1 Polarization Profiles for $\delta > 0$	79
	4.3.2 Polarization Profiles for $\delta < 0$	84
4.4	Thermodynamic Functions	88
4.5	Size Effects and Critical Temperatures	91
4.6	Discussion	98
<b>CHAPTER 5</b>	<b>DIELECTRIC HYSTERESIS LOOPS IN THE SECOND</b>	
	<b>ORDER FERROELECTRIC BILAYERS</b>	<b>101</b>
5.1	Introduction	101
5.2	Formalism for Ferroelectric Bilayer / Superlattice	102
5.3	Spontaneous Polarization in Ferroelectric Bilayer	106
5.4	Hysteresis Loops of Ferroelectric Bilayers and Superlattices	111
5.5	Conclusion	120
<b>CHAPTER 6</b>	<b>HYSTERESIS LOOPS IN THE FIRST ORDER</b>	
	<b>FERROELECTRIC BILAYERS</b>	<b>122</b>
6.1	Introduction	122
6.2	Formalism	123
6.3	The Critical Temperatures	125
6.4	Polarization Profiles	129

6.5	Dielectric Hysteresis Loops	133
6.6	Conclusion	146

**CHAPTER 7 DIELECTRIC HYSTERESIS LOOPS OF  
ANTIFERROELECTRICS**

**149**

7.1	Introduction	149
7.2	Formalisms of First and Second Order AFE	150
7.2.1	Formalism of Second Order AFE	151
7.2.2	Formalisms of First Order AFE	152
7.3	Dielectric Hysteresis Loops of First and Second Order AFE	153
7.3.1	Dielectric Hysteresis Loops of Second Order AFE	154
7.3.2	Dielectric Hysteresis Loops of First Order AFE	160
7.4	Conclusion	171

**CHAPTER 8 SUMMARY AND GENERAL REMARKS ON POSSIBLE  
EXTENSIONS**

**175**

8.1	Summary of New Results	175
8.2	Possible Extensions	179

**REFERENCES**

**181**

**APPENDICES**

**APPENDIX A LIST OF SOME FERROELECTRIC AND  
ANTIFERROELECTRIC COMPOUNDS**

**195**

<b>APPENDIX B</b>	<b>DETAILS OF NUMERICAL CALCULATIONS</b>	
	<b>IN CHAPTER 4</b>	<b>197</b>
<b>APPENDIX C</b>	<b>DETAILS OF NUMERICAL CALCULATIONS</b>	
	<b>IN CHAPTER 5, 6 AND 7</b>	<b>199</b>
<b>LIST OF PUBLICATIONS</b>		<b>201</b>

## LIST OF SYMBOLS AND ABBREVIATIONS

$P_1, P_2$	average polarization in layer 1 and 2 of a bilayer
$k_B$	Boltzmann constant
$E_C$	coercive field
$S_i^z, S_j^z$	components of pseudo-spin
$n_0$	coordinate number
$T_C$	critical temperature
$L_C$	critical thickness
$C$	Curie constant/heat capacity
$T_0$	Curie-Weiss temperature
$\epsilon_r(T)$	dielectric constant at temperature $T$
$\epsilon_r(0)$	dielectric constant at zero temperature
$\xi_l$	displacement variable
$\mathbf{D}$	electric displacement vector
$\mathbf{E}$	electric field vector
$\mathbf{P}$	electric polarization vector
$G$	energy integral
$g$	energy integral in reduced unit
$\Sigma/S$	entropy
$J_{ij}$	exchange strength

$e$	external electric field in reduced unit
$\delta$	extrapolation length
$\pi_l$	general momentum for cell $l$
$J$	interlayer coupling constant
$j$	inter-layer coupling constant in reduced unit
$\alpha, \beta, \lambda$	Landau coefficients
$V(\xi_l)$	local potential function
$\tan \gamma$	loss factor
$\lambda$	modulus of elliptic function
$\Lambda$	periodicity in superlattice
$\epsilon_0$	permittivity of free space
$\mathbf{K}$	reciprocal lattice vector
$P_r$	remanent polarization
$\langle S^z \rangle$	spin expectation value
$P_s$	spontaneous polarization
$\mathbf{x}$	strain tensor
$\mathbf{X}$	stress tensor
$t_{sc}$	supercooling temperature in reduced unit
$t_{sh}$	superheating temperature in reduced unit
$\xi$	temperature dependence of coherent length
$t$	temperature in reduced unit
$t_c$	thermodynamic critical temperature in reduced unit
$l$	thickness ratio (in bilayer), thickness in reduced unit (thin film)
$\Omega$	transverse field

$t_2$	upper limit of field induced temperature in reduced unit
$q$	wave vector
$\xi_0$	zero temperature value of coherent length
ADP	ammonium dihydrogen phosphate, $\text{NH}_4\text{H}_2\text{PO}_4$
AFE	antiferroelectric
BTO	barium titanate, $\text{BaTiO}_3$
CMOS	complementary metal oxide semiconductor
CVD	chemical vapour deposition
DHL	dielectric hysteresis loop
FE	ferroelectric
FERAM	ferroelectric random access memory
IMTF	Ising model in a transverse field
KDP	Potassium dihydrogen phosphate, $\text{KH}_2\text{PO}_4$
LB	Langmuir-Blodgett method
LCD	liquid crystal display
LD	Landau Devonshire
MBE	molecular beam epitaxy
MFA	mean field approximation
MFNOS	metal-ferroelectric-nitride-oxide-semiconductor
MFS	metal-ferroelectric-semiconductor
MOCVD	metal organic chemical vapour deposition
MOD	metal organic deposition
NVRAM	non-volatile random access memory

PLAD	pulse laser ablation deposition
PTO	lead titanate, $\text{PbTiO}_3$
PZO	lead zirconate, $\text{PbZrO}_3$
PZT	lead zirconate titanate, $\text{PbZr}_{1-x}\text{Ti}_x\text{O}_3$
SBT	strontium bismuth titanate, $\text{Sr}_x\text{Bi}_{2-x}\text{Ti}_2\text{O}_9$
SEM	scanning electron microscopy
STO	strontium titanate, $\text{SrTiO}_3$
TEM	transmission electron microscopy
TGS	triglicine sulphate, $(\text{CH}_2\text{NH}_2\text{COOH})_3 \cdot \text{H}_2\text{SO}_4$
TO	transverse optical



## Chapter 1

### AN OVERVIEW

#### 1.1 Introduction

As a mean-field-type theory, Landau theory lacks microscopic perspectives, but it has been successful in describing the phenomenological behaviour of phase transitions in materials like superconductors and ferromagnets. Devonshire, who capitalized on the analogous behaviour of ferroelectrics to ferromagnetic materials, developed the Landau theory to study ferroelectricity using a thermodynamic approach. Ever since then, Landau Devonshire (LD) theory has been an important theoretical tool used in studying the phenomena of first and second order phase transitions in bulk ferroelectrics (FE), and this theory has also been extended to studies of thin films and multilayers.

Since the 1990s, the technology of fabrication in material science has advanced rapidly, and this enhances the ability to produce better quality FE thin films and multilayers or superlattices. In consequence, a wide range of applications of FE thin films and multilayers or superlattices has been found. One of the most exciting applications of FE thin films is in fabricating non-volatile random access memory (NVRAM), where data stored will not be lost when electric field is suddenly cut off. However, there are many problems relating to various applications of FE thin films or superlattices still remaining unresolved; some of these problems pertain to

shortcomings in techniques of fabrication and others are related to insufficient understanding of the physics of FE thin film and multilayers.

The physics of FE thin film surface and size effects and related properties, for instance, the depolarization effect on the surface in contact with another surface, domain formation, switching of dipole moments *etc.*, has been the subject of active studies in ferroelectricity. However, there is still a lot to be done especially on the properties of thin films and superlattices, both experimentally and theoretically. Among the theoretical approaches, LD theory has been popular; and this may be attributed to many creditable results being produced in the studies of properties of bulk FE and thin film FE. Quite recently, the theory has also been extended into the studies of superlattices. In this dissertation, we utilize the LD model to study the phase transition properties of second order FE thin films and the dielectric hysteresis loop (DHL) patterns of FE bilayers of first and second order materials. An overview of the thesis is given in the following section.

## **1.2 Overview of the Thesis**

To present a more complete picture, general reviews of the basic physics of ferroelectrics and of previous work which is related to our studies are given in chapter 2 and chapter 3. A literature review on the fabrication of FE thin films and superlattices and experimental results which relate to the properties of films and superlattices is given in chapter 3. A discussion of previous work on the application of the LD model and the Ising Model in a Transverse Field (IMTF) in studies of FE thin films and superlattices is also included in chapter 3; this has been the source of our motivation. Chapter 4 gives a detailed discussion of the second order phase transition in FE thin films modelled by an extension of LD theory which includes the spatial variation and

surface effect; some calculations on the film profile, critical length and the thermodynamic parameters are included. We devote chapter 5 to modelling a bilayer of second-order FE materials using the LD expression. By varying the thickness ratio and the interlayer coupling, different patterns of DHLs are drawn. The FE bilayer discussed in chapter 6 is modelled from the LD expression of the bulk first order phase transition with some simplifications assumed. Unequal thickness ratio characterizes the most general first order FE bilayer; it forms the subject of discussion in chapter 6. We obtain a great variety of patterns in the DHLs of the first order bilayer by varying the thickness ratio and the interlayer coupling. The LD free energy describing a bilayer with equal thicknesses is the same as that of a two-sublattice bulk antiferroelectric (AFE), so our results for this special case apply to the AFE. While the second-order AFE is discussed in textbooks, a full account of the first-order AFE is not available. Chapter 7 is therefore devoted to the properties, including DHLs, of both second and first order AFEs. Conclusions and possible extensions to the work are presented in chapter 8.

## Chapter 2

### AN OVERVIEW ON BULK FERROELECTRICS

#### 2.1 Introduction

The unusual dielectric properties of Rochelle salt (sodium potassium tartrate tetrahydrate,  $\text{NaKC}_4\text{H}_4\text{O}_6 \cdot 4\text{H}_2\text{O}$ ) were reported by Pockels in 1894 (Kanzig, 1957). But, more intense study of Rochelle salt was aroused only after Valasek (1920, 1921) had reported that the dielectric properties of Rochelle salt are analogous to the magnetic properties of ferromagnetic materials. Busch and Scherrer (1935) later discovered a new ferroelectric crystal in potassium dihydrogen phosphate,  $\text{KH}_2\text{PO}_4$  (KDP). Not long after that, Mueller (1940a, b, c, d) put forward a phenomenological theory that relates the anomalous dielectric, piezoelectric and elastic behaviours of Rochelle salt. The pace of development in the study of ferroelectricity was quickened from the beginning of 1940's where barium titanate ( $\text{BaTiO}_3$ ) and several isomorphs of  $\text{BaTiO}_3$  were found to behave as ferroelectrics. Microscopic theory of phase transitions for KDP and  $\text{BaTiO}_3$  was developed gradually by Slater (1941, 1950); and that further enhanced the enthusiasm among physicists in the study of ferroelectricity. In 1949, Devonshire (1949) published a theory on the phase transition mechanism of  $\text{BaTiO}_3$ . His theory has deepened the understanding on the behaviour of  $\text{BaTiO}_3$  and has initiated the thermodynamic theory in ferroelectricity. An important breakthrough in the study of

ferroelectricity came from Cochran (1959) and Anderson (1960) when they independently proposed the soft mode theory on the phase transitions of ferroelectrics.

Zhong (1998a) briefly classifies the history of ferroelectric studies into four stages. It began with the discovery of Rochelle salt and the KDP series between 1920 and 1939. From 1940 to 1958, the phenomenological theory of ferroelectricity was established and developed into maturity. The development of the ferroelectric soft mode theory occupied the duration from 1959 to 1970. From 1980 onwards until now, major studies are focused on various types of non-equilibrium ferroelectric systems. Mitsui and Nakamura (1990) reported that the number of ferroelectrics known to date has exceeded 200 (a ferroelectric compound or solid solution in mixtures or by substitution of its constituent ions is not considered as a new ferroelectric).

The general properties of the bulk ferroelectric, including the basic concept of spontaneous polarization and the general definition of ferroelectricity are discussed in Section 2.2. Then we present in Section 2.3 the types of ferroelectric materials and the basic concepts of ferroelectric phase transitions. Microscopic and macroscopic theories of ferroelectric phase transitions including the soft mode theory and Landau Devonshire theory are briefly discussed in Section 2.4. Finally, a brief outline on the applications of the ferroelectric materials is delivered in Section 2.5.

## **2.2 Bulk Ferroelectric Properties**

Besides the classification of crystals into seven Bravais systems according to their geometry, crystals are also classified into 32 point groups according to their symmetry with respect to a point. Among the 32 point groups, 11 of them possess a centre of symmetry, and the remaining 21 are non-centro-symmetric. Piezoelectric crystals are those without a centre of symmetry. These classes of crystals exhibit electric polarity

when they are subjected to stress and strain or to applied electric field. Among the 21 non-centro-symmetric point groups, 20 are piezoelectric crystal classes. Polarization is a vector quantity, and the existence of spontaneous polarization in a crystal creates a unique direction or axis whereby the whole crystal is polarized. This polarized axis is not equivalent to any of the symmetric axes of the crystal and it is called the unique polar axis. It is discovered that only ten out of the 20 piezoelectric crystal classes have a unique polar axis and exhibit spontaneous polarization. These 10 polar crystal classes are often called the ferroelectric crystals. So it is obvious that all ferroelectric crystals are piezoelectrics, but the converse is not true.

Ferroelectric phase transition is a structural phase transition. As a result of transition from the high temperature phase, a spontaneous polarization appears and some symmetry elements of the high temperature phase are lost on cooling below the transition temperature  $T_C$ . We can define the spontaneous polarization either as a quantity of surface density of a bound charge on the sample surface or the permanent dipole moment per unit volume in the crystal. In another perspective, the spontaneous polarization is due to the relative displacement of atoms (ions) in a phase transition. We describe a ferroelectric crystal as a polar crystal, whose spontaneous polarization  $P_S$  can be in two or more orientational states in the absence of an electric field. The direction of the spontaneous polarization  $P_S$  can be switched to another state by an applied electric field greater than the coercive field  $E_C$  (shown in Fig 2.3).

Pyroelectric effect, i.e. the dependence of  $P_S$  on temperature, exists in ferroelectric crystals, and the 10 ferroelectric crystal classes are also called the pyroelectric classes. Since the atomic arrangement in the crystal varies with temperature and the atomic displacement in the crystal is related to spontaneous polarization  $P_S$ ,

thus  $P_s$  is temperature dependent. In the absence of an electric field,  $P_s$  varies non-linearly with temperature  $T$  below the Curie temperature  $T_C$ . In typical ferroelectrics, the spontaneous polarization decreases as temperature increases and it disappears continuously or often discontinuously at  $T_C$ . The nature of this continuous or discontinuous jump in the spontaneous polarization at  $T_C$  depends on the order of the phase transition. For the second-order phase transition the spontaneous polarization goes to zero continuously at  $T_C$ . While, there is an abrupt jump in spontaneous polarization to zero at  $T_C$  for the first-order phase transition. Fig. 2.1 shows typical

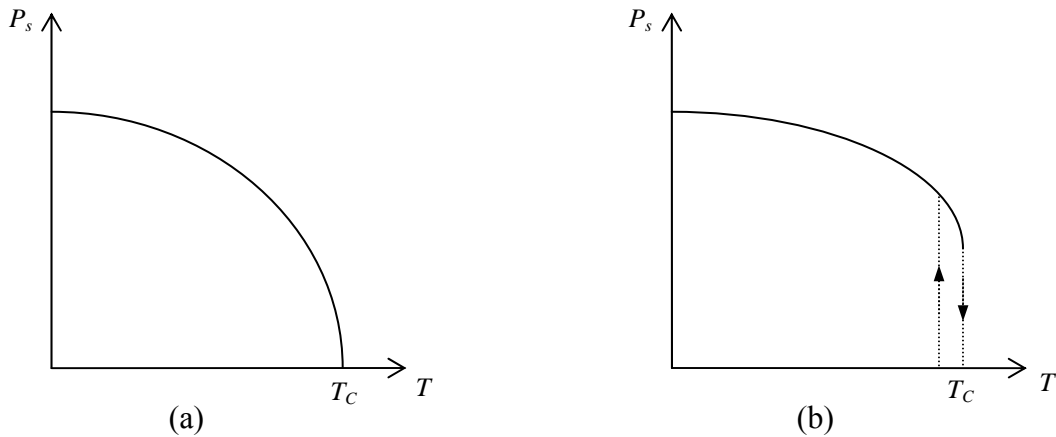


*Fig. 2.1 The change of spontaneous polarization,  $P_s$  with temperature  $T$  for: (a) second-order and (b) first-order phase transition*

cases of the variation of spontaneous polarization with temperature for the first and second-order phase transition at zero field. At this juncture, we observe that  $T_C$  demarcates the whole temperature range into the paraelectric (nonpolar) phase above  $T_C$  and the ferroelectric (polar) phase below  $T_C$ .

Other than these phenomena, there is an anomalous behaviour in dielectric constant at  $T_C$ . Along the direction of the spontaneous polarization in the ferroelectric phase, the temperature dependence of the dielectric constant in the low frequency phase is given by

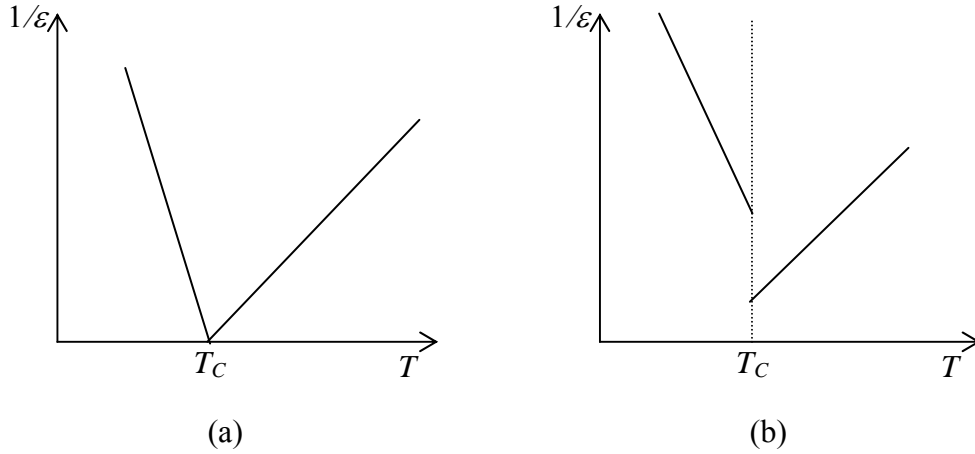


Fig. 2.2 The inverse dielectric constant for: (a) the second-order phase transition; (b) the first-order phase transition.

$$\epsilon_r(T) = \epsilon_r(0) + \frac{C}{T - T_0} \quad (2.1)$$

where  $\epsilon_r(0)$  is the dielectric constant at zero temperature  $C$  is the Curie constant and  $T_0$  is the Curie-Weiss temperature.  $\epsilon_r(0)$  is usually very much smaller than the second term in (2.1) and it is not temperature dependence, hence to a good approximation it can be neglected. Equation (2.1) can then be written as

$$\epsilon_r(T) = \frac{C}{T - T_0} \quad (2.2)$$

We see a divergence in  $\epsilon_r(T)$  at  $T_0$ , where  $T_C = T_0$  for the second-order transitions and  $T_C > T_0$  for the first-order transitions. Fig. 2.2 (a) and 2.2 (b) show the inverse dielectric constant for the second-order and first-order phase transitions respectively.

Below the Curie point, other than the non-linear change in spontaneous polarization with temperature, the other non-linear effect on the spontaneous polarization is due to the applied electric field on the crystal. By plotting the change in polarization with the field, a hysteresis loop resembling the magnetic hysteresis loop is obtained. When the applied field is weak, polarization increases linearly with the field



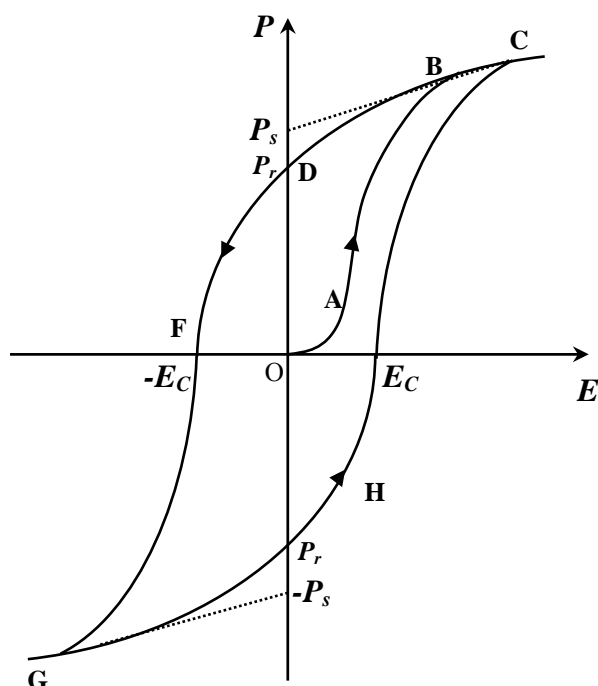


*Fig. 2.3 The dielectric hysteresis loop for a typical ferroelectric crystal.*

and it is because of the dominance of movable domain walls from the newly formed domain nuclei. When the field is increased, the nuclei grow and ultimately the domain walls move irreversibly; polarization increases faster than linearly with the field. This is what we see in curve AB of a typical dielectric hysteresis loop shown in Fig. 2.3. Ultimately, the polarization tends to saturate at B and the crystal is in a single domain. Further increase in applied field increases the total polarization due to the induced polarization by the field. In the contrary, when the field is reduced along CBD, the macroscopic polarization decreases, and in zero field the remanent polarization  $P_r$  remains. But, the extrapolation of CB cuts the vertical axis at a value called the spontaneous polarization  $P_s$ . This is the equilibrium polarization in the ferroelectric phase.

If the field is reversed, polarization continues to decrease, but its direction is not yet reversed. When the reversed field exceeds a value  $E_C$  (coercive field) at F, the crystal polarization changes its direction. At point F, the coercive field  $E_C$  is attained; total polarization in the crystal is made zero. Further increase in the reversed field causes saturation of the reversed polarization shown at G. The portion of the curve DFG shows the changes of polarization as the field is reversed. When the applied field varies from the values along the curve CBDFGHC in a cycle, the hysteresis loop is traced. The hysteresis loop illustrates that the free energy of the crystal is equivalent for the two possible directions of the vector  $P_s$ , and the possibility of switching the spontaneous polarization by an external electric field is evident.

### 2.3 Ferroelectric Materials and Their Properties

According to the phenomenological behaviour of the ferroelectric crystals, we can classify them into displacive type and order-disorder type. This way of classifying ferroelectric materials is discussed in details by Lines and Glass (1977) and Zhong (1998a). Kanzig (1957) discussed two other ways of classifying the ferroelectric materials. He classified ferroelectric materials by the number of axes along which they can be polarized or by considering whether they are piezoelectric in the unpolarized phase. There are a great number of ferroelectric compounds being discovered and studied over the years. There are two texts, which accommodate a table compiled by Subbarao on ferroelectric and antiferroelectric materials discovered, in Lines and Glass (1977) as well as Blinc and Žekš (1974). As a convenient reference on real values of critical temperature of ferroelectric or antiferroelectric materials, a list of selected ferroelectric and antiferroelectric materials with their corresponding critical temperatures is given in appendix A (Blinc and Žekš, 1974; Lines and Glass, 1977).

Burfoot and Taylor (1979) give some discussion on the preparation of ferroelectric materials and it is enlightening to the theorists who might not have a hands-on experience on the materials. This section is allotted for some discussion on the characteristics of the displacive and order-disorder ferroelectrics; in particular properties of barium titanate ( $\text{BaTiO}_3$ ) and potassium dihydrogen phosphate (KDP) are highlighted as the respective examples.

### 2.3.1 Displacive Ferroelectrics

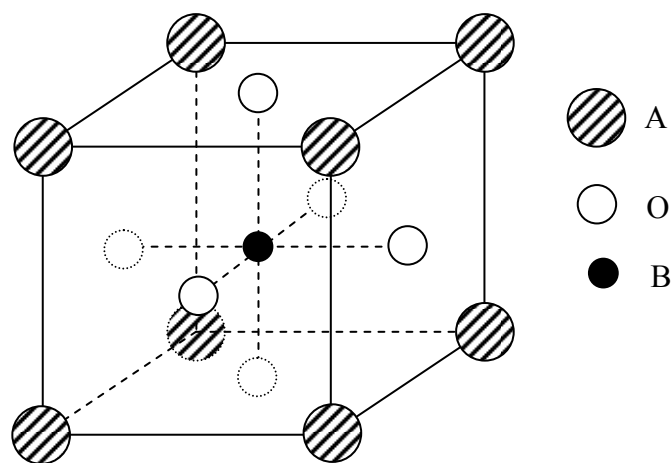
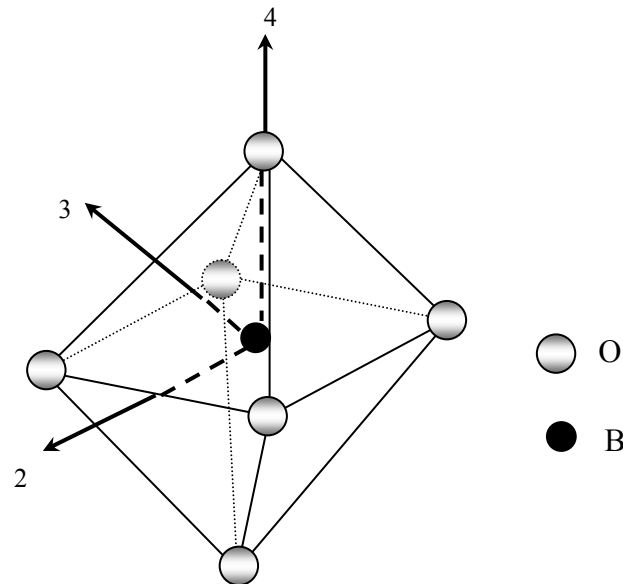


Fig. 2.4 The cubic structure of a perovskite,  $\text{ABO}_3$ .

A displacive ferroelectric undergoes a phase transition whereby the atoms in the crystal begin to displace at the transition temperature, and this leads to a change in crystal symmetry. The perovskite type (such as  $\text{BaTiO}_3$  or  $\text{PbTiO}_3$ ), lithium niobate type (such as  $\text{LiNbO}_3$  or  $\text{BiFeO}_3$ ) and tungsten bronze type (such as  $\text{Ba}_2\text{Sr}_{5-x}\text{Nb}_{10}\text{O}_{30}$  or  $\text{PbTa}_2\text{O}_6$ ) belong to the displacive ferroelectrics. The typical ferroelectric perovskite  $\text{BaTiO}_3$  happens to be the first known ferroelectric perovskite. It was first discovered by Wul and Goldman (Wul and Goldman, 1945a, 1945b 1946) independently. The perovskite structure has a general formula  $\text{ABO}_3$ , where A is a monovalent or bivalent metal ( $\text{A}^+$

or  $A^{2+}$ ), B is a tetra- or pentavalent one ( $B^{4+}$  or  $B^{5+}$ ), and O the oxygen atom. Besides  $BaTiO_3$ , some other examples of ferroelectric perovskites are  $KNbO_3$ ,  $PbTiO_3$ ,  $KTaO_3$  and  $PbZr_xTi_{1-x}O_3$  (PZT). There are also trifluoride type perovskites  $ABF_3$  (example  $KMnF_3$ ) but they are not ferroelectrics and will not be discussed.



*Fig. 2.5 The oxygen octahedron structure with the axes of rotation symmetry. ( 2, 3, 4 means two-fold, three-fold and four-fold axis respectively). (Zhong, 1998)*

The crystal structure of the perovskites is cubic (in the paraelectric phase), with the A atoms at the corners of a cube, B atoms at the centre, and oxygen atoms at the face centres as shown in Fig.2.4. We can see that the oxygen atoms occupy the six vertices of an octahedron with B at its centre. The whole crystal can also be seen as the oxygen octahedral group  $BO_6$  being arranged in a simple cubic structure, with the A atoms occupy the spaces in between. Owing to the octahedron structural of  $BO_6$ , the perovskite type is sometimes known as the oxygen octahedral type. The octahedron consists of three sets of axes of rotation symmetry, namely 3 four-fold axes, 4 three-fold axes and 6 two-fold axes (Lines and Glass, 1977; Zhong, 1998a) as shown in Fig. 2.5. The spontaneous polarization in the perovskite ferroelectrics and the other ferroelectrics that contain the oxygen octahedral group is due to the displacement of the B ions from

its central positions in the octahedron. Normally, the displacement of the B ions is along the direction of one of these three axes, and so is the direction of the spontaneous polarization.

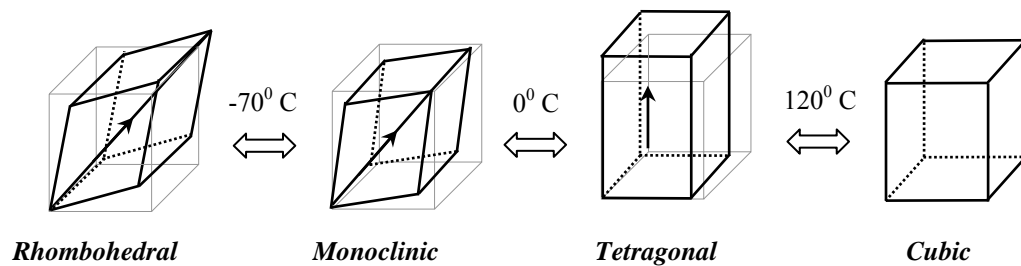


*Fig. 2.6 Structural phase transitions in Barium Titanate, BaTiO<sub>3</sub>.*

As a typical example of displacive ferroelectric, BaTiO<sub>3</sub> is cubic at temperature above  $120^{\circ}\text{C}$  and it is in paraelectric phase. Fig. 2.6 shows the structural phase transitions of BaTiO<sub>3</sub>. If we consider a unit cell of the BaTiO<sub>3</sub>, it contains one formula-unit of BaTiO<sub>3</sub>. At  $120^{\circ}\text{C}$ , it undergoes a paraelectric-ferroelectric phase transition. Below the phase transition temperature ( $T_c = 120^{\circ}\text{C}$ ) the cubic lattice is distorted and the crystal structure is transformed to tetragonal. The atoms shift along the fourfold axes as mentioned above. Hence, the oxygen octahedron is distorted and the unit cell is pulled in the direction of atomic displacement (Fig. 2.7). This means that relative to the paraelectric phase, the Ti<sup>4+</sup> ion shifts in the direction of z-axis, but the O<sup>2-</sup>I and O<sup>2-</sup>II ions move in the negative z-axis direction with Ba<sup>2+</sup> ions assumed stationary. Ferroelectric-ferroelectric phase transition happens at  $0^{\circ}\text{C}$  with the structural change from tetragonal to monoclinic. Another low temperature ferroelectric-ferroelectric phase transition is at  $-70^{\circ}\text{C}$  and its crystal structure shifts from the monoclinic to rhombohedral structure. Fig. 2.8 shows the phase transitions in BaTiO<sub>3</sub> (Strukov and Levanyuk, 1998), and it is shown that at all the three transitional temperatures, there are

discontinuous jumps in  $P_s$ , and these discontinuities in  $P_s$  indicate that the phase transitions are first-order. The earlier phase transition figure for  $\text{BaTiO}_3$  by Merz (1949) printed in most of the ferroelectric texts show that  $P_s$  changes continuously at

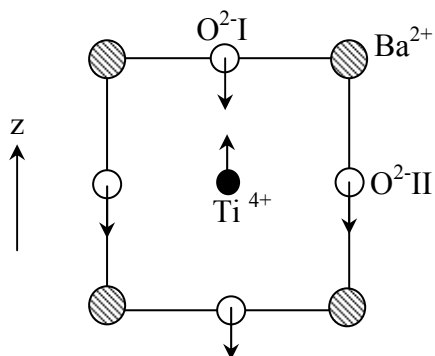


Fig. 2.7 Projection of the  $\text{BaTiO}_3$  structure in the  $(0,1,0)$  plane. Arrows indicate the directions of displacement of  $\text{Ti}^{4+}$  and  $\text{O}^{2-}$  ions.  $\text{Ba}^{2+}$  ions are stationary.

$120^\circ\text{C}$ . In fact, it is the first-order close to second-order phase transition. Nevertheless, in his later measurement using a good crystal, Merz showed clearly that it is indeed discontinuous at the critical temperature of  $120^\circ\text{C}$  (Merz, 1953). In a first-

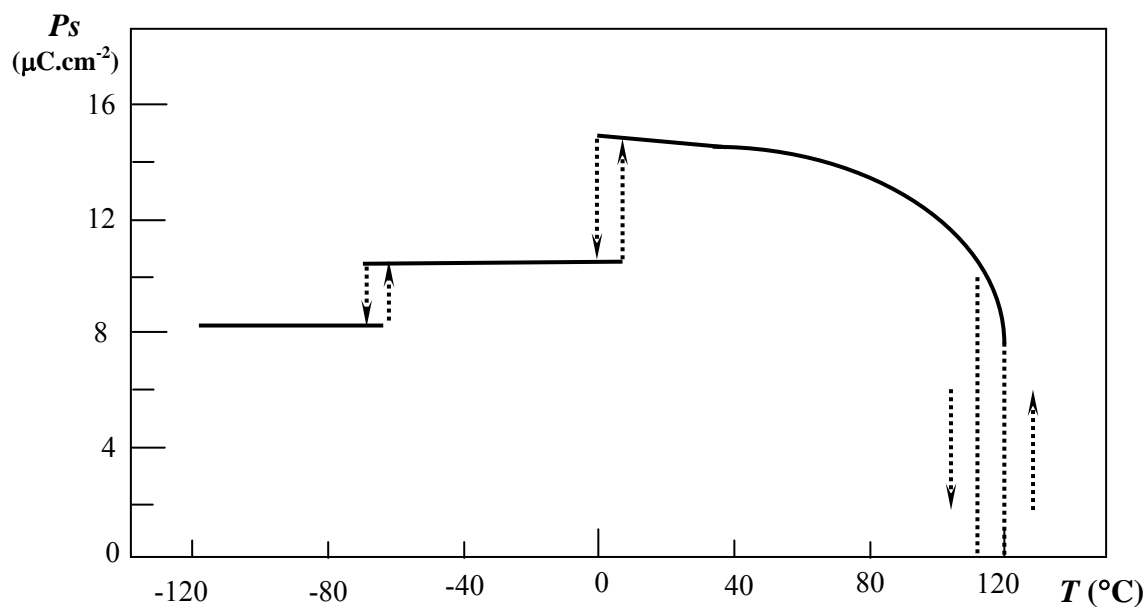


Fig. 2.8 Temperature dependence of spontaneous polarization in  $\text{BaTiO}_3$  (Strukov and Levanyuk, 1998)

order ferroelectric, a double hysteresis loop is expected between  $T_C$  and  $T_{Critical}$  (which is  $T_{SH}$  in our notation). Merz (1953), in his same paper showed the hysteresis loops of  $BaTiO_3$  for a series of temperatures (Fig. 2.9). Some discussion on the phenomenological theory of the phase transitions of  $BaTiO_3$  by Devonshire is found in the text by Mitsui *et al.* (1976). Lines and Glass (1977) give a very comprehensive review on the materials, which contain the oxygen octahedral group from the experimental and theoretical perspectives.

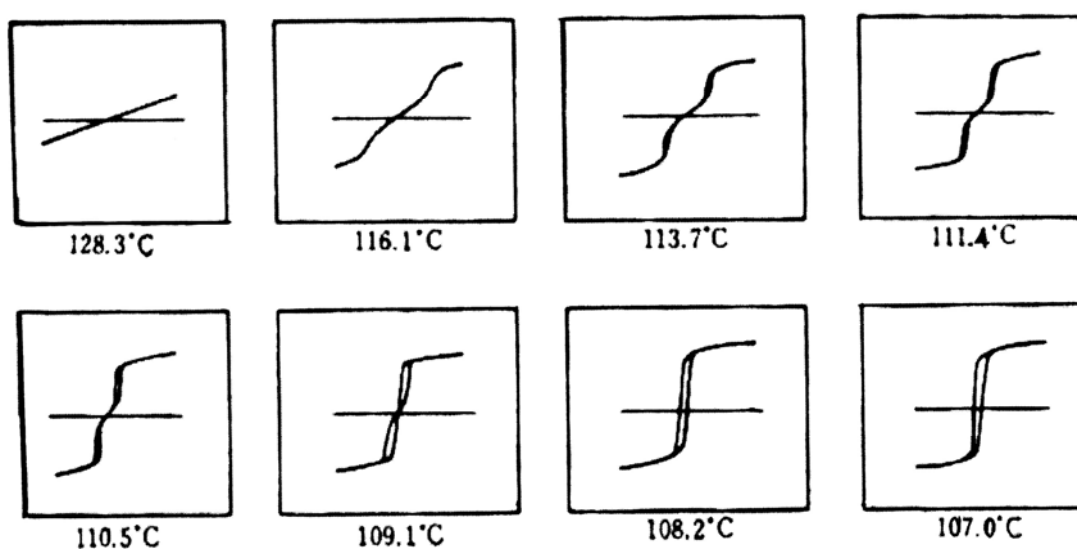
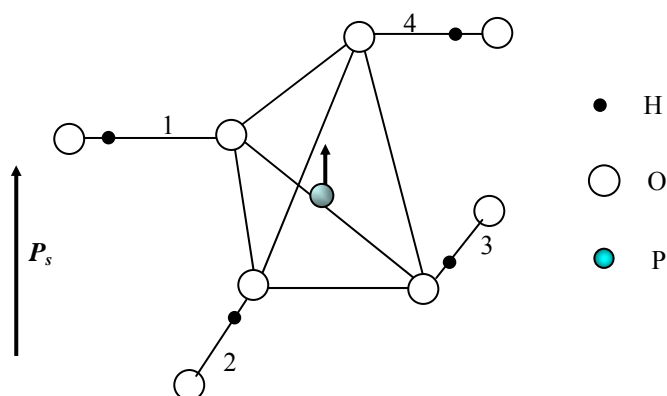


Fig. 2.9 Hysteresis loops of  $BaTiO_3$  for a series of temperatures (Merz, 1953)

### 2.3.2 Order-Disorder Ferroelectrics

There is no sharp demarcation between the displacive and order-disorder phase transitions in term of structural phase transitions. In the order-disorder phase transitions, there is a change in the crystal symmetry as a result of the redistribution of the particles or ions over equiprobable positions at the transition temperature. In comparison with the displacive ones, the crystal structures of the order-disorder ferroelectrics are more complex. The typical examples of crystalline order-disorder

ferroelectrics include sodium nitrite ( $\text{NaNO}_2$ ), potassium dihydrogen phosphate (KDP,  $\text{KH}_2\text{PO}_4$ ) and triglycine sulphate (TGS,  $(\text{CH}_2\text{NH}_2\text{COOH})_3\cdot\text{H}_2\text{SO}_4$ ). There are other



*Fig. 2.10 The system of hydrogen bonds in  $\text{KH}_2\text{PO}_4$  (KDP) crystal: the  $\text{PO}_4$  tetrahedron with hydrogen bonds to the nearest neighbours*

KDP ferroelectric isomorphs like rubidium dihydrogen phosphate (RDP),  $\text{RbH}_2\text{PO}_4$  and  $\text{KD}^*\text{P}$  the deuterated form of KDP, where the hydrogen atoms in the KDP are replaced by deuterium ( $^2_1\text{H}$ ). Other KDP-type arsenates like  $\text{KH}_2\text{AsO}_4$  (KDA),  $\text{RbH}_2\text{AsO}_4$  (RDA) and  $\text{CsH}_2\text{AsO}_4$  (CDA) are found to possess ferroelectric transitions of first-order (Blinic, Burgar, and Levstik, 1973). Ammonium dihydrogen phosphate (ADP) is a KDP-type antiferroelectric (Nagamiya, 1952). Among all those crystals, the KDP and TGS are the most thoroughly studied. In the order-disorder ferroelectrics, below the transition temperature, the ordering takes place in a sub-lattice and it displaces the atoms in other sub-lattices. Thus, the spontaneous polarization is due to the displacement of ions that do not belong to the sub-lattice that is being ordered and it measures the amount of long range ordering of permanent dipoles. There are many order-disorder ferroelectrics that contain hydrogen bonds, and the hydrogen atom is



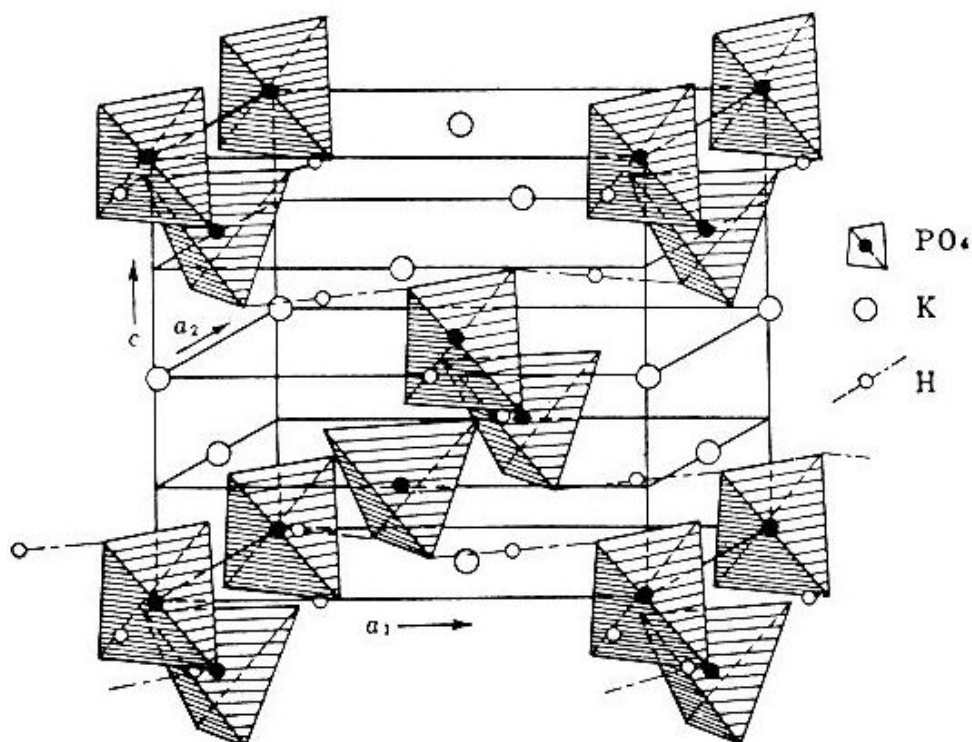


Fig. 2.11 The structure of the  $\text{KH}_2\text{PO}_4$  (KDP) crystal.

next to the strongly electronegative atoms oxygen, nitrogen, fluorine, and chlorine; typical examples are KDP and TGS.

The transition temperature of KDP is at 123 K, and its crystal symmetry changes from the tetragonal (above  $T_C$ ) to orthorhombic structure (below  $T_C$ ). Above  $T_C$ , the crystal structure consists of  $\text{K}^+$  ions and almost regular tetrahedral  $\text{PO}_4^{3-}$  groups. The  $\text{P}^{5+}$  ions are located at the centres of the tetrahedral  $\text{PO}_4^{3-}$  groups. The  $\text{P}^{5+}$  ions lie above the  $\text{K}^+$  ions on the fourfold axes separated by half the unit cell parameter in the direction of z-axis. Each tetrahedral  $\text{PO}_4^{3-}$  group links to four other tetrahedral  $\text{PO}_4^{3-}$  groups via the O-H...O bonds (Fig. 2.10). The two upper oxygen atoms of the  $\text{PO}_4^{3-}$  group are attached to the two other tetrahedra on the same level, and the lower two oxygen atoms of the same  $\text{PO}_4^{3-}$  group are attached to another two tetrahedra on the same level. This gives rise to a net of  $\text{PO}_4^{3-}$  groups linked with the symmetrical

hydrogen bonds, O-H...O. The whole net of hydrogen bonds is almost parallel to the (001) plane. The structure of the KDP crystal above  $T_C$  is depicted in Fig. 2.11. (Zhong, 1998a; Strukov and Levanyuk, 1998; Lines and Glass, 1977).

The ordering of the protons on the hydrogen bonds in the KDP does not directly contribute to the spontaneous polarization of the crystal, but the interaction of protons with  $K^+$  and  $P^{5+}$  ions causes the displacement of the  $K^+$  and  $P^{5+}$  ions that induces the spontaneous polarization. Above  $T_C$ , the proton is situated randomly at the two equilibrium positions along the hydrogen bond length, as the two equilibrium positions have the energy level represented by a symmetrical double-well potential. However, below  $T_C$ , the protons are more ordered. They are mainly found in one of the two positions along the hydrogen bond, which means that they can be located nearer to the upper (or lower) oxygen atoms of the  $PO_4^{3-}$  groups. Since the orientation of the dipoles in the hydrogen bonds attached to the tetrahedra is perpendicular to the z-axis, there is no contribution to the spontaneous polarization. Nevertheless, the ordering of protons in the hydrogen bonds induces the displacement of  $K^+$  and  $P^{5+}$  ions along the z-axis in the opposite direction and this induces the spontaneous polarization in the crystal (Bacon and Pease, 1953).

## 2.4 Theory of Ferroelectric Phase Transitions

The development of the phenomenological theory of ferroelectricity began well in 1940; Mueller (1940a, b, c, d) proposed a phenomenological theory pertaining to the understanding of the anomalous behaviours of Rochelle salt. After the discovery of  $BaTiO_3$ , Ginzburg (1945, 1949) and Devonshire (1949, 1951, 1954), accomplished the development of thermodynamic theory of ferroelectric phase transitions. Kittel (1951) then further extended the theory into the phase transitions of antiferroelectrics. The

thermodynamic theory of ferroelectric phase transitions was fundamentally matured in the 1950's (Zhong, 1998a). However, the development of microscopic theory was still a struggle. Slater proposed the first molecular theory on the ferroelectric transition of  $\text{KH}_2\text{PO}_4$  (KDP) (1941) and  $\text{BaTiO}_3$  (1949) based on the actual crystal structure. He proposed that the phase transitions in  $\text{BaTiO}_3$  and KDP were due to the displacement of Ti atom at the centre of the oxygen octahedron and the ordering of proton on the hydrogen bond respectively. The major breakthrough came from Cochran and Anderson. They proposed that the ferroelectric phase transitions should be studied within the framework of crystal dynamics, and to focus on the lowering of frequency in the TO (transverse optical) mode (soft mode) during phase transition. The 'freezing-in' of the soft optical phonon causes the static atomic displacement and thus, induces the spontaneous polarization (Cochran, 1959; Anderson, 1960). In his later publications (Cochran, 1960, 1961, and 1963), Cochran systematically illustrated the above idea. Soft mode theory reveals the characteristic of ferroelectric phase transitions. The theory indicates that the ferroelectric (and antiferroelectric) phase transition is a special case of a structural phase transition. This theory was quickly confirmed by experiments and has enhanced the development of the physics of ferroelectricity.

#### **2.4.1 Soft Mode and Microscopic Theory**

The soft mode theory was initially applied in the displacive structures like  $\text{BaTiO}_3$ . Later, it was found that the same ideas can also be used in the order-disorder systems like  $\text{KH}_2\text{PO}_4$  (De Gennes, 1963; Brout *et al.*, 1966). The fundamental concept of the soft mode theory in a displacive ferroelectric is that, on approaching the critical temperature  $T_C$ , the frequency of the soft phonon decreases and the restoring force for the mode displacement tends to zero (the short range force balances the long range

Coulomb force) as the soft phonon is 'frozen' at  $T_c$ . The static atomic displacements (from the high temperature phase to the low temperature phase) represent the 'frozen-in' mode displacements of the unstable phonon. The static component of the unstable phonon is the spontaneous polarization. The soft phonon, in this case, must be polar and of long wavelength ( $\mathbf{q} \rightarrow 0$ , where  $\mathbf{q}$  is the wave vector). In other words, the ferroelectric phase transition involves the 'freezing-in' of a soft phonon at the Brillouin zone centre ( $\mathbf{q} = 0$ ). On the other hand, the antiferroelectric soft phonon has a finite wavelength due to the presence of two opposite sub-lattice polarizations. Thus, the antiferroelectric phase transition involves the 'freezing-in' of soft phonon at the Brillouin zone boundary ( $\mathbf{q} = \mathbf{K}/2$ , where  $\mathbf{K}$  is a reciprocal lattice vector). The mechanism of the soft mode discussed above is applied to the displacive system. It is different in the order-disorder system because the soft mode is no longer the instability of soft phonon but it is the unstable pseudo-spin wave which describes the displacement of the protons within the double-potential-well-like hydrogen bonds.

Irrespective of the difference in the mechanism of the phase transitions in the displacive ferroelectrics and hydrogen bonded ferroelectrics in general, the phase transitions in ferroelectrics (or antiferroelectrics) are usually related to the rearrangement of a few atoms in the unit cell and the positions of the other atoms remain unchanged. We can see this from the examples in  $\text{BaTiO}_3$  where Ti ion is displaced with respect to the oxygen octahedron in the unit cell, and in KDP where the proton is rearranged in the double well potential of the O-H--O hydrogen bond. Thus, in the study of soft mode dynamics of the ferroelectrics, it is only necessary to take into account of the motion of these particular coordinates and treat the other coordinates in the crystal lattice as a heat bath (Lines, 1969; Thomas, 1971).

With this in mind, there is a great simplification in the construction of the theory based on the local-mode. The basic Hamiltonian (Lines and Glass, 1977) for a solid can be written as follow:

$$H = H(\text{ion}) + H(\text{electron}) + H(\text{electron - ion}) \quad (2.3)$$

where  $H(\text{ion})$  describes interactions of the ion centres,  $H(\text{electron})$  describes the valence electron motion, and  $H(\text{electron - ion})$  describes the interactions between valence electrons and ion cores. The states of electrons are assumed to be just a function of the ionic coordinates, further approximation is made by making assumption that the potential energy of interacting valence electrons and the ion cores is independent of the electron configuration or of temperature. The resulting Hamiltonian includes the relative motion of the rigid ion cores and the valence electrons for each ion (Cochran, 1960, 1961). Finally, the dynamic of the ionic system describes in the local-mode approximation in the simple model Hamiltonian (Lines and Glass, 1977) can be shown in general as:

$$H = \sum_l \left\{ \frac{1}{2} \pi_l^2 + V(\xi_l) \right\} - \frac{1}{2} \sum_l \sum_m v_{lm} \xi_l \xi_m \quad (2.4)$$

where  $\pi_l$  is the generalized momentum for cell  $l$  with displacement variable  $\xi_l$  and  $V(\xi_l)$  is the local potential function that can be in any form from quasi-harmonic to deep double-well form; while  $v_{lm} \xi_l \xi_m$  is the bilinear two body interaction potential which may be either short range or long range or both. An electric field of static or time-dependent form can also be added to the Hamiltonian (2.4). The above equation in general facilitates the statistical problem of obtaining the solutions of the phase transitions of the ferroelectrics or antiferroelectrics. Nevertheless, even for the most simplified form of the Hamiltonian, there is no exact solution; and the simplest approach to this statistical problem is by taking the mean-field approximation (MFA).

In the MFA the interaction of the particles is described as an average field acting on each particle and the field is assumed to be independent of position in the lattice.

We have presented a brief qualitative discussion on the simple model Hamiltonian on the theory of ferroelectric phase transition. The detailed quantitative discussion of the simple Hamiltonian and the mean-field solutions can be found in some standard ferroelectric texts (Zhong, 1998a; Lines and Glass, 1977; Blinc and Zēks, 1974).

The theory behind the occurrence of spontaneous polarization in the order-disorder ferroelectrics can be illustrated by the ordering of proton on the double-well-potential hydrogen bond in the hydrogen-bonded ferroelectrics like KDP. The displacement of the proton between these two wells and its possibility of tunneling through can be described by the pseudo-spin wave theory, which is a matured theory in the study of ferromagnetism. The two possible states of a proton in the double-well potential are analogous to the spin up and spin down states of spin  $\frac{1}{2}$  particle. The interactions between neighbouring double-wells are treated as the exchange coupling between these pseudo-spins. The model Hamiltonian based on this pseudo spin is the Ising model. The tunneling probability through the well can be incorporated into the Hamiltonian by representing it with a transverse field. The final model Hamiltonian is known as Ising Model in a Transverse Field (IMTF). The mean-field solutions of this model have successfully explained the empirical phenomena among which it has predicted the isotopic effect between KDP and  $\text{KD}^*\text{P}$  (deuterated form of KDP) excellently. It is not our purpose to discuss the qualitative aspects of the theory but just to give an overview about the subject. For the details, one can refer to the standard texts of Zhong (1998), Lines and Glass (1977) or Blinc and Zēks (1974).

### 2.4.2 Landau Devonshire Theory

As we have mentioned in the earlier section, ferroelectric phase transition is a type of structural phase transition. The concept of structural phase transition, which relates to the breaking of symmetry accompanied by a change in the order parameter, was proposed by Landau. The breaking of symmetry means that one or more symmetry elements of the crystal suddenly appear or disappear across the transition temperature. Before we go into the thermodynamic theory of ferroelectricity by Devonshire (which is more generally known as Landau Devonshire theory), it is more complete to give a brief discussion on the Landau theory.

According to Landau theory (Landau and Lifshitz, 1980; Izumov and Syromyatnikov, 1990), the change in the symmetry elements of a system undergoing a structural phase transition can be studied via the change in the 'density function'  $\rho_0(x, y, z)$  of the system, where  $\rho_0(x, y, z)$  determines the probabilities of the different positions of the crystal above the Curie point. The symmetry of the crystal lattice is determined by the space group  $\mathbf{G}_0$ , in which all the coordinate transformations leave  $\rho_0(x, y, z)$  invariant. By cooling the crystal slightly below  $T_C$ , some of the symmetry elements of  $\mathbf{G}_0$  disappear, and the density function of the crystal will be written as:

$$\rho(x, y, z) = \rho_0(x, y, z) + \delta\rho(x, y, z) \quad (2.5)$$

where  $\delta\rho(x, y, z)$  is the small change in the density function. The resulting density function  $\rho(x, y, z)$  and the small change  $\delta\rho(x, y, z)$  should be invariant under a group  $\mathbf{G}_1$  and logically  $\mathbf{G}_1$  must be a subgroup of  $\mathbf{G}_0$ . It is known from the group theory that the density function  $\rho(x, y, z)$  can be represented as a linear combination of some other functions, which are invariant under the symmetry group  $\mathbf{G}_1$ . These functions can be chosen in the form of sets of as few functions as possible. Each set of functions

is invariant under the transformations of the group. The matrices that transform the functions in each set form the irreducible representations of  $\mathbf{G}_1$ .

Usually two different phase transitions (at different temperatures) are represented by changes in symmetry corresponding to two different independent irreducible representations. Thus, it can be assumed that in the second-order phase transition,  $\delta\rho(x, y, z)$  corresponds to a single irreducible representation in  $\mathbf{G}_0$  as:

$$\delta\rho(x, y, z) = \sum_i C_i \varphi_i(x, y, z) \quad (2.6)$$

where  $\varphi_i(x, y, z)$  is a basis function of the irreducible representation and  $C_i$  are the coefficients of the basis functions. The actual values of  $C_i$  are determined thermodynamically; for instance, at  $T_c$  the symmetry of the crystal is  $\rho_0(x, y, z)$  and all  $C_i$  must be zero. So,

$$\delta\rho(x, y, z) = 0, \quad \rho(x, y, z) = \rho_0(x, y, z), \quad T = T_c \quad (2.7)$$

In continuous, i.e. second-order, phase transitions  $\delta\rho(x, y, z)$  must vanish continuously and so  $C_i$  must take small values since they vanish when  $T_c$  is approached. Hence the free energy density can be expanded in Taylor's series in powers of  $C_i$  near  $T_c$ . With the substitution of  $C_i$  by  $\eta\gamma_i$  and having

$$\sum_i \gamma_i = 1 \quad (2.7)$$

the free energy density can now be in terms of  $\eta$ , the order parameter; where  $\gamma_i$  are the symmetry parameters. More explicitly, we can say that through Landau Theory, the structural phase transition of a ferroelectric is described in terms of even powers of an order parameter  $\eta$  which appears at  $T_c$  when the symmetry of the paraelectric phase is broken. In ferroelectrics,  $\eta$  is the spontaneous polarization which vanishes above  $T_c$



and is non-zero below  $T_C$ . Further details in obtaining the phenomenological equation describing the ferroelectric phase transitions can be found in the texts by Tolédano and Tolédano (1987) and Blinc and Zeks (1974).